INVESTIGATIONS ON THE HEAT TRANSFER DURING PFC-MELTSPINNING BY ON LINE HIGH SPEED TEMPERATURE MEASUREMENTS

Andreas Ludwig and Georg Frommeyer

Max-Planck-Institut für Eisenforschung GmbH
Department of Materials Science and Technology
Postfach 140444
4000 Düsseldorf, Germany

Abstract

To evaluate the heat transfer coefficient h between the solidifying ribbon and the wheel surface during the formation of FeSi 5 wt.% melt spun ribbons by Planar Flow Casting, high speed surface temperature measurements of the melt pool and of the solidifying ribbon have been carried out by using a rotating fiber optical system. The recorded cooling curves have been interpreted by computer simulations. A comparison of the measured and the calculated cooling curves shows that for the melt pool almost ideal cooling conditions occur ($h \geq 5 \cdot 10^6$ W/m^{2}K). During the solidification of a thin layer, the heat transfer coefficient changes to lower values of about $4 \cdot 10^4$ W/m^{2}K at the beginning of the process and to about $12 \cdot 10^4$ W/m^{2}K after several wheel revolutions. Thus the cooling of the solidified ribbon becomes more efficient with increasing process time although the wheel surface temperature increases. The decrease in h during the solidification is caused by a lift up of grain boundary areas. The results of the numerical modelling reveal that the solidification is related to the shape of the measured cooling curves. Therefore it can be shown that ribbons of 100 to 200 μm in thickness are solidified within a time interval of 2 to 3 ms, resulting in an average growth rate of 10 - 60 mm/s. This leads to a fine dendritic structure with diminishing microsegregation.

presented at the symposium
'Melt-spinning and Strip Casting'
on the TMS Annual Meeting
San Diego, march 1992

Introduction

For melt spinning and related rapid solidification processes the heat transfer plays a key role in the development of fine grained microstructures resulting from a high growth velocity of the solidification front. The melt spin process offers the possibility of getting information about the cooling history of rapidly solidifying materials by measuring the ribbon surface temperature. For the interpretation of the measured cooling curves a substantial understanding of the solidification process with respect to the undercooling at the wheel-ribbon contact zone, the corresponding temperature gradient in the solid and the liquid zone and the resulting growth rate will be obtained.

Several attempts have been made to measure the cooling rate curves of the melt puddle surface during the formation of microcrystalline melt spun ribbon, comparing the appearing temperature distribution with appropriate models. H.A. Davies et al. [1,2] used photocalorimetry to determine the cooling curves during the solidification of crystalline ribbons. They evaluated their results with an analytical approximation. B. Cantor et. al [3,4] applied the same technique and determined the heat transfer coefficient by an analytical expression as well as a numerical simulation. Vogt et al. [5,6] used a set of fast response infrared pyrometer and interpreted the results with a finite difference algorithm taking the latent heat of fusion and the heating of the wheel into account. The authors found evidences that the heat transfer coefficient is not constant during the solidification process. Mühlbach et al. [7] applied thermovision measurements and compared the results with an effective specific heat method based on a finite difference simulation. They found that the evaluated cooling curve can be well understood by considering a decrease in the heat transfer coefficient from $h \approx 10^8$ W/m^2K (ideal cooling condition) to about $h \approx 10^4$ W/m^2K. No physical explanation was given for the decrease in h.

In the present paper a new fibre optical system for detecting the temperature radiation of rapidly solidifying ribbons with a measuring frequency of 50 kHz on the base of high speed double pyrometry will be described. To evaluate the obtained cooling curves a numerical model has been developed, which takes into account the melt undercooling at the wheel contact zone as well as the KGT-theory for constrained dendritic growth [8]. The calculations showed that the solidification is related to the shape of the measured cooling curves. A decrease in h has also been found. By SEM-investigation of the contact side topology of melt spun ribbons an interpretation of the reduction in the heat transfer coefficient is given. In addition the average growth rate and the time interval for the completed solidification of FeSi 5 wt.% melt spun ribbons, 100 - 200 μm in thickness, have been determined and the effect of the growth rate on the morphology and the appearing microsegregations is considered.

Experimental Procedure

A rotating mirror-lens-system, connected at the casting wheel, is used to register the temperature radiation from the middle zone of the melt puddle and the solidifying ribbon. The fiber optic diverts the radiation to a coupling on the wheel axes. From there it is reflected into a second optical fiber which guides the signal into a double pyrometer. There the radiation is divided into two optically equivalent rays which are registered at different wavelengths by photodiodes. The wavelength selection is performed by two interference filters. Using a 100 Ω input resistance, the intensity of the temperature radiation, which is proportional to the photovoltage of the diode, is trapped and amplified with low noise operational amplifiers. The

obtained data were stored simultaneously by a transient recorder. From the measured voltages the temperature was calculated by applying the basic equation for double pyrometry.

During the casting process the rotating mirror-lens-system passes the nozzle/melt pool area frequently and reflects the temperature radiation of a 2 mm^2 spot size from the middle of the wheel surface into the optical system. When the temperature radiation of the melt is detected, the photovoltages of the two diodes increase to more than the default trigger level of 4 V which starts the storage of the detector signals. The reading is completed after a time period of 20 ms. After one wheel rotation the trigger level is again exceeded, starting another measurement of the temperature radiation. This technique enables the on-line recording of numerous cooling curves in constant process time intervals.

The response time of the photodiodes and of the transient recorder is less than 500 ns and that of the operational amplifiers is on the order of 20 μs. Thus the amplifiers are the time limiting devices in this measuring system. Using a fast luminescence diode a maximum measuring frequency of 50 kHz for the electronic system was estimated. Further details concerning the mechanical and electrical components of this system or the theoretical background of the temperature determination is given in [9].

For investigating the melt undercooling at the wheel contact zone and the non-equilibrium solidification of a crystalline phase, temperature measurements have been carried out during the production of FeSi 5 wt% melt spun ribbons. With wheel velocities between 8 and 15 m/s ribbons of 100 to 200 μm in thickness and 30 mm in width have been produced. The melt spinning facility for the ribbon production and technical details, concerning the process, are described in [6].

The measured cooling curves have been evaluated by using a suitable numerical model, which is based on the two-dimensional thermal transport equation. In this model the heat release during solidification is taken into account by a source term similar to the 'effective specific heat capacity technique'. An explicit finite difference method on a rectangular grid fitted to the melt puddle geometry has been applied. The heat transfer at the melt-wheel interface is described by a heat transfer coefficient h_1, whereas the heat transfer between the solidifying ribbon and the roller is defined by a second heat transfer coefficient h_2. The heat radiation of free surfaces is neglected.

It is stated that the solidification starts with a surface induced heterogeneous nucleation at the melt-wheel interface. Since the parameter determining the heterogeneous nucleation and especially the transient effects (which may be important at high cooling rates [10]) are generally not known, the undercooling necessary for the nucleation is treated as an external parameter. The growth rate during the solidification process has been estimated due to the KGT-theory [8] for constrained dendritic growth with high Péclet-numbers. Microsegregation has been treated by the model of Giovanola and Kurz [11], which has been extended up to the solute limit of stability. For further details of the numerical model the reader is referred to [12,13].

Results

Fig.1 exhibits three successive cooling curves measured during the production of a 130 μm thick ribbon with a wheel surface speed of 10 m/s. The curves are marked due to the chrono-

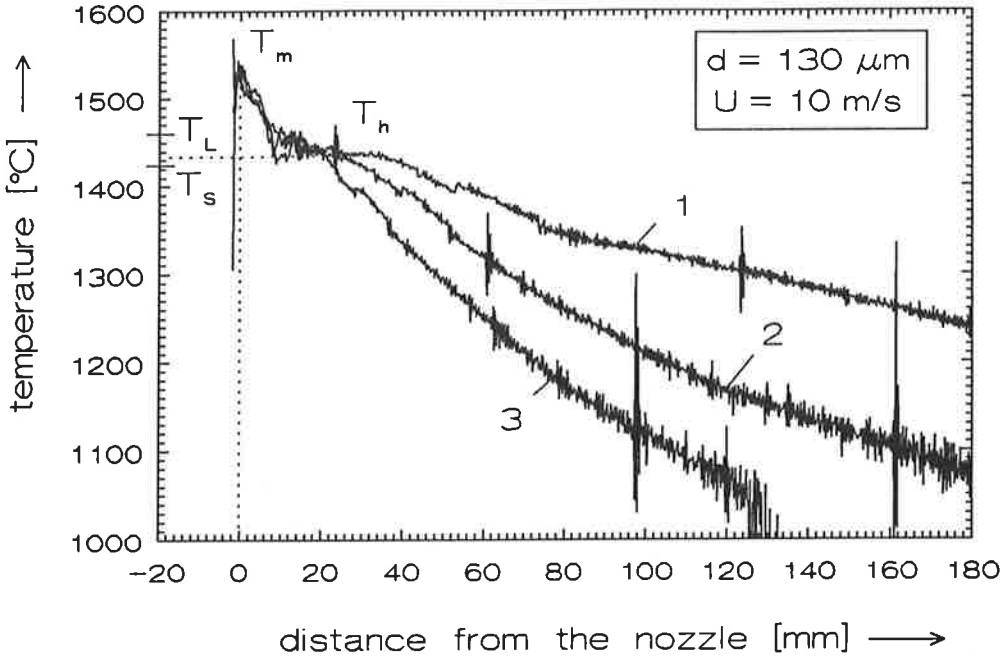

Fig.1. Cooling curves of three successive solidification processes marked due to the chronological order. (T_m: maximum-, T_h: plateau-, T_L: solidus-, T_S: liquidus temperature)

logical order. Starting from a maximum at $T_m \simeq 1520°C$, the temperature decreases to a temperature plateau at $T_h \simeq 1440°C$, which is in the interval between the liquidus and solidus line of the FeSi 5 wt.% alloy. T_m is related to the rear edge of the nozzle, where the melt leaves the nozzle-wheel-gap. After remaining at T_h for a period of about 2 - 3 ms, which corresponds to a distance of 20 - 30 mm from the rear edge of the nozzle, the temperature decreases again continuously. In the high temperature regime no significant differences occur. Whereas below the temperature plateau at T_h the curves reveal considerable dissimilarities. The overall cooling rates increases from $T \simeq 1.5 \cdot 10^4$ K/s for the first curve to $T \simeq 3.7 \cdot 10^4$ K/s for the third one. Although the temperature of the preheated wheel increases from 200°C at the beginning of the casting process to about 450°C after three wheel revolutions, the cooling becomes more efficient with increasing process time.

Because of the limited amount of melt (about 300 g) in the crucible for the production of 100 to 200 µm thick ribbons, 30 mm in width, with a wheel speed of 10 m/s, the casting process is completed after about 1 s, which results in about six successive wheel revolutions. This allows six repeating cooling runs to be measured. All studied casting processes experienced an improvement of the cooling behaviour as demonstrated by the steeper slope of the cooling curves, presented in fig.1. Thus for the performed casting experiments no steady state is achieved during the process time. Further on, due to the strong influence of the wheel surface temperature and the surface oxidation on the cooling rate and the heat transfer, it was not possible to obtain identical cooling curves by using the same process parameters. Even a thin ribbon experience lower cooling rates than a thicker one, if the wetting due to an oxidized wheel surface is deteriorated.

However the temperature curves, represented in fig.1, are characteristic for the solidification of FeSi 5 wt.% melt spun ribbons, 100 - 200 µm in thickness, produced with wheel speeds between 8 and 15 m/s. Typical recalescence phenomena like undercooling and successive

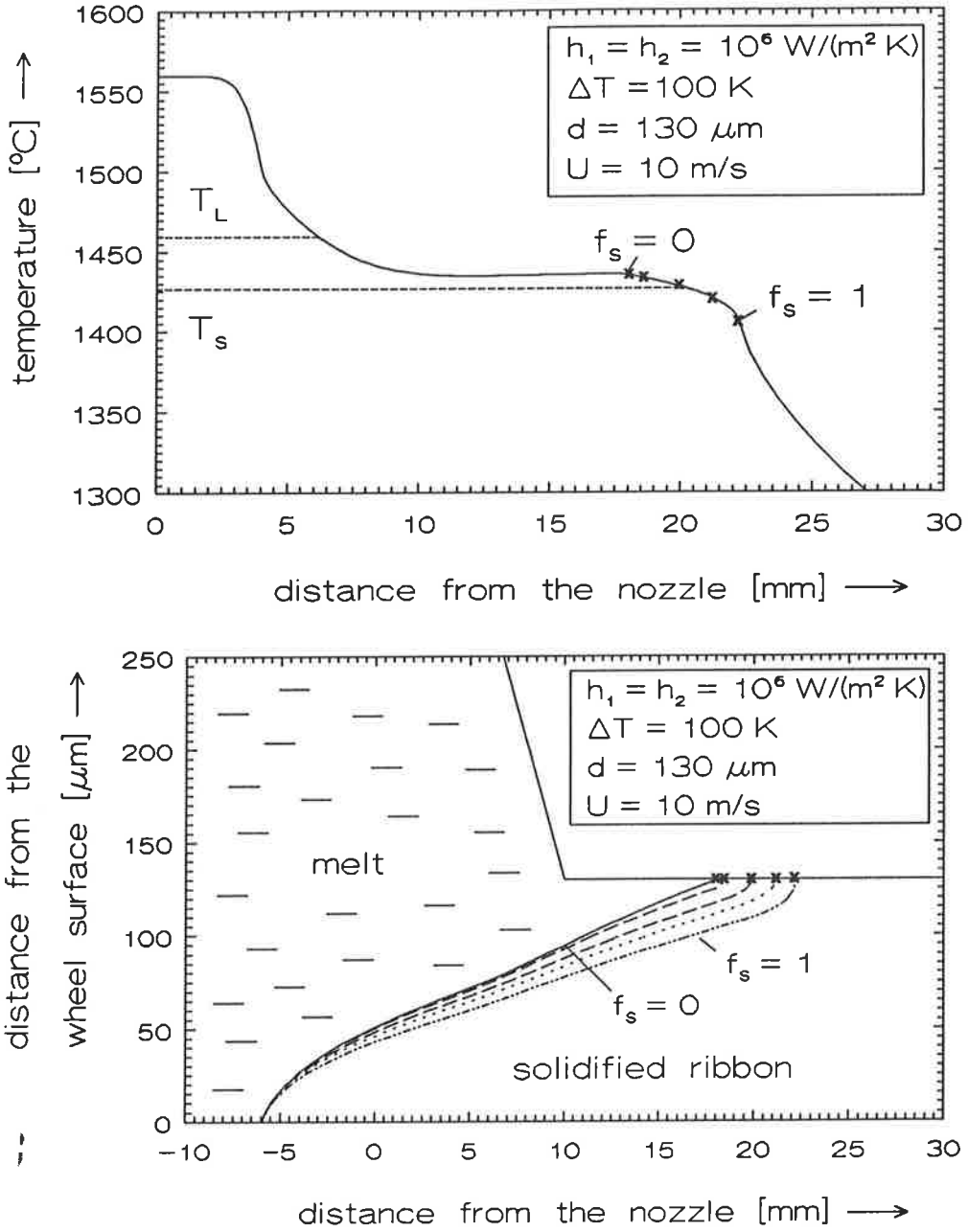

Fig.2. a) Calculated cooling curves with marked area of the solidifying ribbon surface for the given process parameters. b) Cross section of the melt pool were the ribbon is formed, with plotted mushy zone. f_s describes the volume fraction of the solidified melt.

heating were not observed on the surface of the melt pool and the solidifying ribbon, respectively. Average cooling rates calculated from the measured cooling curves for the temperature interval from T_m to 1100°C are in the order of $10^4 - 6 \cdot 10^4$ K/s.

Extensive studies of the influence of different process parameters on the surface temperature of the melt pool and the solidifying ribbon by using numerical process simulations reveal that the solidification is related to the shape of the measured cooling curves. Fig. 2a shows a calculated cooling curve where the area of solidifying ribbon surface is marked. Analogous

to the measurements, the calculated surface temperature decreases from the temperature of the slightly superheated melt to a constant plateau temperature. For comparison, fig. 2b exhibits a cross section through the melt pool with the plotted mushy zone. The solidification starts due to a surface induced heterogeneous nucleation with a planar liquid-solid interface. Due to the latent heat release the interface temperature increases, leading to a growth rate lower than the limit of absolute stability for the constrained growth condition. Therefore the growth morphology changes from planar to dendritic. The corresponding mushy zone is indicated by doted lines which represents the relative amount of solid from $f_S = 1$ for the dendrite roots to $f_S = 0$ for the dendrite tips.

Both figures are based on a calculation for a FeSi 5 wt.% ribbon, 130 μm in thickness, with a heat transfer coefficient of $h_1 = h_2 = 10^6$ W/(m^{2}K) and a wheel surface speed of $U = 10$ m/s. A melt undercooling at the wheel contact zone of $\Delta T = 100$ K was taken into account. The shape of the melt pool has been approximated by a straight line with a total length of 10 mm and the melt pool expansion under the nozzle was estimated to be 10 mm.

A comparison of the results, illustrated in figure 2a and 2b reveals, that when the dendrite tips reach the top of the melt pool the temperature will decrease under the plateau temperature. The solidification of the interdendritic melt is complete when the temperature remain under the solidus line. Estimating the length of the temperature plateau of the measured cooling curves the solidification time and for a defined ribbon thickness an average growth rate can be calculated. For example FeSi 5 wt.% melt spun ribbons, 100 - 200 μm in thickness, solidify within 2 to 5 ms (fig.1) with an average solidification velocity of 10 - 60 mm/s.

Discussion

For evaluating the heat transfer coefficient the measured cooling curves have been compared with theoretical predictions of the numerical process simulation. In spite of an extensive parameter study it was not possible to fit the measured cooling curves for the temperature range from T_m to 1100°C considering only one constant heat transfer coefficient. The calculated curves reveal a faster cooling compared with the experimental observations. This discrepancy may be explained by a decrease in the heat transfer between the solidifying ribbon and the wheel. In the numerical simulation the reduced heat transfer has been considered by changing the heat transfer coefficient from a high value h_1 to a lower one h_2. This has been performed when the distance from the dendrite tips to the wheel surface exceeds $d_X = 50$ μm. Fig.3 shows two cooling curves, measured during the production of a 110 μm thick ribbon, with the appropriate calculated temperature distributions. The heat transfer coefficients used for the calculations are specified in the diagram.

To interpret the decrease in the heat transfer during the solidification of a thin layer in contact to the wheel, SEM-investigations of the ribbon contact surface have been performed. In addition to the frequently observed air pockets [14], the contact surface of the ribbon exhibits a fine network of smooth areas (Fig.4) on the boundaries of the grains which are in contact to the wheel while on the middle part of this grains the profile of the wheel surface is marked.

Due to the high heat transfer coefficient of the melt-wheel interface of about $h_1 = 5 \cdot 10^6$ W/(m^{2}K) ideal cooling between the melt and the substrate has to be considered. When nuclei

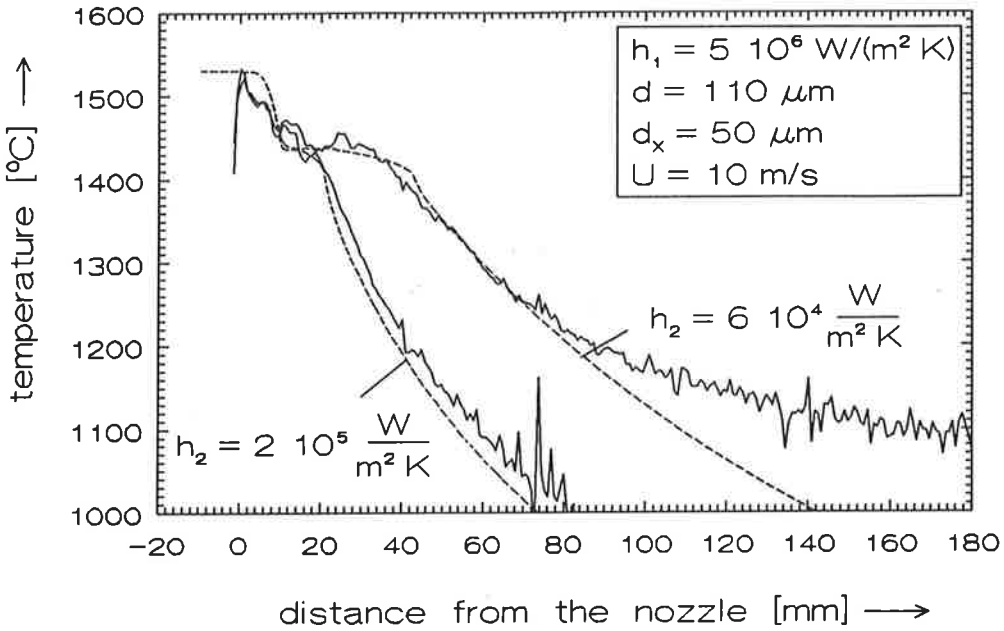

Fig.3. Comparison of the measured and the calculated cooling curves. To fit the experimental curves, h_1 had to be reduce to h_2 after primary solidification of a layer at the wheel-ribbon contact zone, $d_x = 50\,\mu m$ in thickness.

are formed by surface induced heterogeneous nucleation the solidification of separate grains take place in strong contact with the wheel surface. Due to the volume shrinkage of the solidifying grains the melt between the grains is lifted up, resulting in the smooth topology of the grain boundary areas. Hence the effective contact area decreases. The heat transfer coefficient can be interpreted as a macroscopical quantity, which averages over an adequate contact area. The decrease in the contact area results in a reduction of the heat transfer coefficient. Thus the discontinuous change in h used in the process simulation has to be interpreted as a first approximation.

Casting the molten alloy on a wheel with a surface temperature of about 200°C results in a large change of h during the solidification from about $h_1 = 5 \cdot 10^6\,W/(m^2K)$ to about $h_2 = 6 \cdot 10^4$ $W/(m^2K)$ (fig.3), two orders of magnitude. During the casting the substrate surface is heated up. Using a mild steel wheel the surface temperature increases during the production of microcrystalline ribbons, 100 - 200 μm in thickness and 30 mm in width of about 30 - 50°C per wheel rotation. Thus a wheel surface temperature of about 600°C occurs within 1 s. Casting under this conditions results in a change in h from about $h_1 = 5 \cdot 10^6\,W/(m^2K)$ to about $h_2 = 2 \cdot 10^5\,W/(m^2K)$ (fig.3). The wheel temperature does not effect the heat transfer between the melt and the substrate, but it strongly influences the heat transfer between the solidifying ribbon and the wheel.

This result is identical to the correlation between the heat transfer coefficient and the substrate temperature reported by R.E. Maringer [15]. He found in his drop-splat experiments a critical sticking temperature T_c for a substrate, where the metallic droplets stick on the inclined substrate surface after solidification. The value of T_c differs for each melt-substrate pair. He argued that if the substrate temperature is higher than T_c, stresses in the solidified splats induced by thermal contraction can be relaxed, either in the droplets or in the substrate, and therefor a release stress is not developed. In addition to this interpretation it

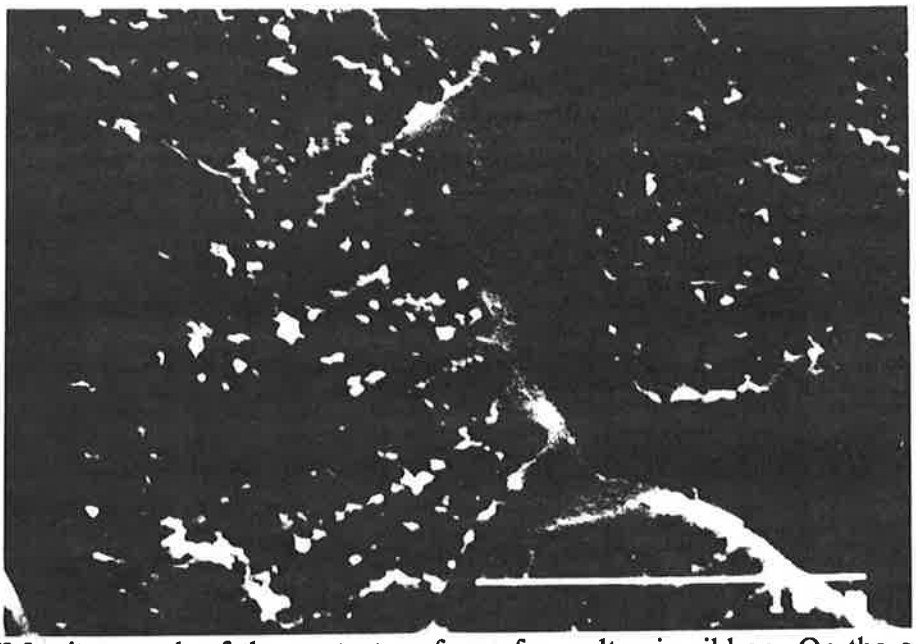

Fig.4. SEM-micrograph of the contact surface of a melt spin ribbon. On the grain surfaces the profile of the wheel surface is marked.

has to be taken into account that an oxide layer on the wheel surface is piled up during the process. By each wheel rotation the lifting ribbon removes partly the oxide layer which has been build up during the preheating of the wheel. For a better understanding of the mechanisms of the heat transfer during the casting process further investigations have to be carried out in greater details.

Relating the solidification time of 2 to 5 ms with the ribbon thickness results in an estimation of an average growth rate on the order of 10 - 60 mm/s. Compared with the upper limit of absolute stability for directional growth, which is about 280 mm/s for the FeSi alloy, the estimated growth rates are extremely high and should result in a fine dendritic or cellular growth morphology and diminishing microsegregations [16]. This corresponds well with the observed cellular microstructure of the ribbon and some fine dendrites on the ribbon surface [17,18]. Compared with conventional casting processes, where growth rates on the order of 1 μm/s are common, the high solidification rate during PFC-meltspinning leads to reduced microsegregations and a suppression of the B2 and DO_3 ordering phases in FeSi melt spun ribbon [19].

Acknowledgment

The authors are grateful to the Deutsche Forschungsgemeinschaft for financial support under Contract No. Fr. 543/7.

References

1. M.J. Tenwick and H.A. Davies, Proc. 5th Int. Conf. on Rapidly quenched Metals, ed. S. Steeb and H. Warliment (Elsevier, 1985), 67 - 70

2. H.A. Davies, Proc. 5th Int. Conf. on Rapidly quenched Metals, ed. S. Steeb and H. Warliment (Elsevier, 1985), 101 - 106

3. A.G. Gillen and B. Cantor, Acta. Metall. 3 (1985), 1813-1825

4. B.P. Bewlay and B. Cantor, Int. J. of Rapid Sol. 2 (1986), 107-123

5. E. Vogt and G. Frommeyer, Proc. ASM Conf. on Rapidly Solidified Materials , San Diego, February 1986, 291-297

6. E. Vogt, Int. J. of Rapid Sol., 3 (1987), 131-146

7. H. Mühlbach, G. Stephani, R. Sellger and H. Fiedler, Int. J. of Rapid Sol., 3 (1987), 83-89

8. W. Kurz, B. Giovanola and R. Trivedi, Acta Metall. 34 (1986), 823-830

9. A. Ludwig and G. Frommeyer, Steel Research, submitted for publication

10. K.F. Kelton and A.L. Greer, J. Non-Cryst. Solids 79 (1986), 295-309

11. B. Giovanola and W. Kurz, Metal. Trans. A 21 (1990), 260-264

12. L. Gránásy and A. Ludwig, Proc. of the Int. Conf. on Solidification and Microgravity Miskoly, Hungary (1991), in print

13. A. Ludwig, L. Gránásy and G. Frommeyer, to be published

14. S.C. Huang and H.C. Fiedler, Met. Trans. A 12 (1981), 1107-1112

15. R.E. Maringer, Mater. Sci. Eng. 98 (1988), 13-20

16. W. Kurz, D.J. Fischer, Fundamentals of Solidification (3 ed. Trans Tech Publications, Aedermannsdorf, 1989)

17. E. Vogt and G. Frommeyer, Z. Metallkde. 78 (1987), 263-267

18. A. Ludwig, (Ph.D. Thesis, Technical University Aachen, 1992)

19. J.E. Wittig, E. Vogt and G. Frommeyer, Ultramicroscopy 30 (1989), 172-180